ACS EARTH AND SPACE CHEMISTRY

http://pubs.acs.org/journal/aesccq

Article

Can Isoprene Oxidation Explain High Concentrations of Atmospheric Formic and Acetic Acid over Forests?

Michael F. Link, Tran B. Nguyen, Kelvin Bates, Jean-François Müller, and Delphine K. Farmer*

Cite This: *ACS Earth Space Chem.* 2020, 4, 730−740

Read Online

ACCESS | Metrics & More | Article Recommendations | Supporting Information

ABSTRACT: Formic and acetic acid concentrations are particularly high over forested areas of the world. However, the gas-phase mechanisms for producing these acids are poorly understood even for isoprene, the globally dominant biogenic hydrocarbon. We quantified formic and acetic acid production from reactions of hydroxyl radical (OH) (between high and low ranges of nitric oxide (NO) levels) with isoprene, methacrolein (MACR), isoprene epoxydiol (IEPOX), isoprene hydroxy hydroperoxide (ISOPOOH), and α-pinene from the focused isoprene experiments at California Institute of Technology (FIXCIT) laboratory chamber study. We find that (i) OH oxidation of MACR, IEPOX, and ISOPOOH are sources of formic acid, (ii) isoprene peroxy radical isomerization and associated photolysis oxidation products are potentially important sources of organic acids, and (iii) high levels of NO generally suppress organic acid formation from OH oxidation of isoprene. We modified existing chemical mechanisms for isoprene oxidation to account for organic acid production pathways observed in the FIXCIT study. We simulated organic acid production during the Southeastern Oxidant and Aerosol Study using the updated chemical mechanisms and represented acetic acid within a factor of 2 but still underpredicted formic acid by a factor of 6. While we cannot explain ambient formic acid with explicit chemical mechanisms, the FIXCIT results suggest that the oxidation of isoprene could account for as much as 70% of the global annual production of formic acid from gas-phase reactions.

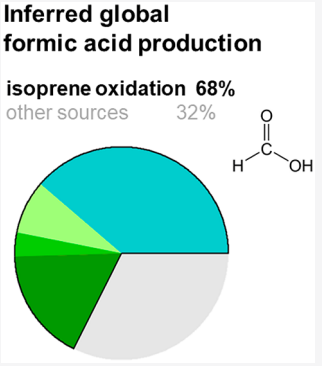

KEYWORDS: *formic acid, isoprene, photochemical oxidation, environmental chambers*

INTRODUCTION

Formic (HCOOH) and acetic (CH_3COOH) acid are the two most abundant gas-phase organic acids in the atmosphere and control important atmospheric processes such as regulation of rainwater pH and gas-particle partitioning.[1,2] In fact, formic acid alone may contribute 30−50% to rainwater acidity in the southeastern United States in the summertime.[3] A recent surge in the interest in atmospheric organic acids is due in part to new instrumentation for both in situ and remote detection that have enabled multiple model-measurement comparisons.[3−6] These comparisons consistently show a missing source of formic and acetic acid, particularly over regions of heavy biogenic influence.[3,5,7,8] This gap in our understanding of organic acid sources is intriguing because organic acids represent a key fate of hydrocarbons emitted into the atmosphere with potential impacts on aerosol formation.

Secondary chemistry of precursors from biogenically dominated environments has been singled out as the principle source of formic and acetic acid to the global atmosphere.[5,7,9] Primary emission sources, such as soils or plants, have been repeatedly demonstrated to be insufficient to explain upward formic acid fluxes from forested environments;[10,11] instead upward fluxes have been associated with isoprene or monoterpene oxidation.[12] Isoprene, emitted mostly from broadleaf trees in forested environments, is the most important source of reactive nonmethane carbon to the atmosphere and is hypothesized to be a major source of formic acid.[3] Lack of targeted laboratory studies of formic and acetic acid formation from isoprene oxidation has been cited as a major reason why models do not constrain organic acid production well.[7,12]

Extensive ambient measurements of isoprene and its oxidation products were taken during the Southeastern Oxidant and Aerosol Study (SOAS) in the summer of 2013 in Talladega National Forest in Alabama. High levels of formic acid were observed during SOAS and the temporal behavior indicated a rapid photochemical source and depositional sink.[13,14] To understand the SOAS observations, the Focused Isoprene eXperiment at the California Institute of Technology (FIXCIT) included a series of chamber experiments to study isoprene oxidation under a variety of SOAS-relevant environmental conditions and oxidants. Here, we present formic and acetic acid yields from these experiments and use models of isoprene oxidation to evaluate potential mechanisms leading to organic acid formation.

Received: January 10, 2020
Revised: March 29, 2020
Accepted: March 30, 2020
Published: March 30, 2020

https://dx.doi.org/10.1021/acsearthspacechem.0c00010
ACS Earth Space Chem. 2020, 4, 730−740

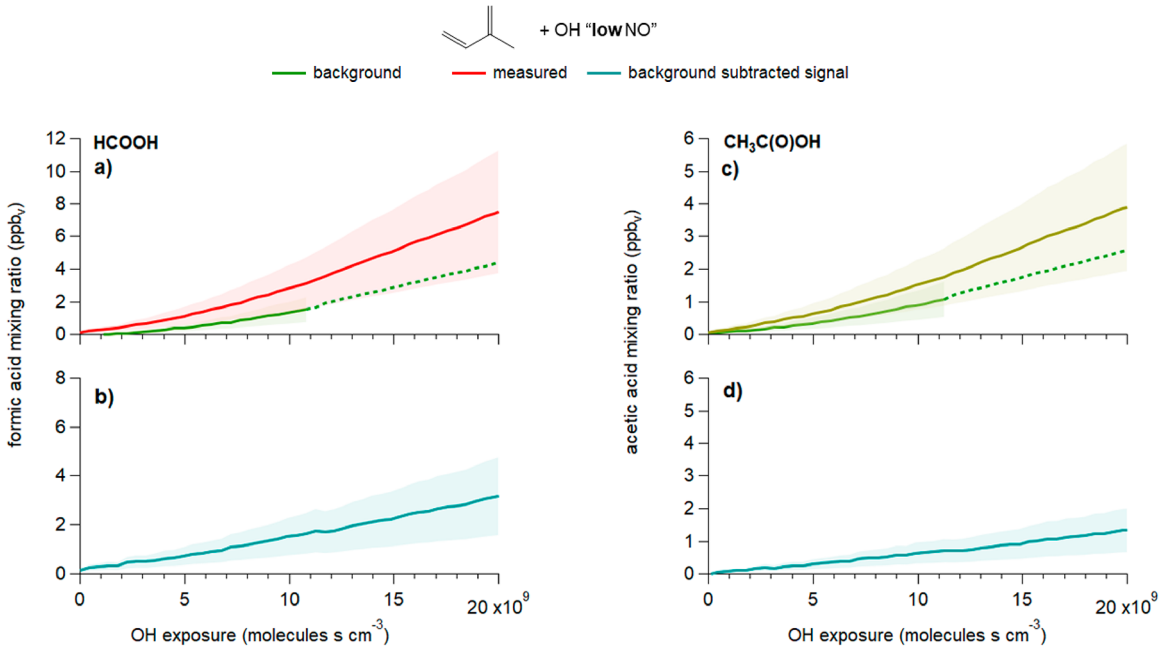

Figure 1. An example of background subtraction of formic (a,b) and acetic (c,d) acid from the isoprene + OH low NO experiment as a function of OH exposure (molecules s cm^{-3}). (a,c) The measured organic acid mixing ratio (red) is shown with the estimated background (green). The solid line represents the direct measurement of background, while the dashed line represents the interpolated mixing ratio (end point for interpolation not shown). (b,d) Subtracting the background from the measured organic acid results in the background-subtracted formic acid mixing ratio for the isoprene + OH low NO experiment (blue line). Shaded regions represent measurement uncertainty.

EXPERIMENTAL METHODS

Gas-Phase Oxidation Experiments. The FIXCIT study consisted of a series of chamber experiments from January 2–30, 2014 and focused on the OH, O_3, and nitrate radical (NO_3) oxidation of isoprene, α-pinene, and specific oxidation products of both precursors. A complete overview of the instrumentation suite, experimental design, and facilities is reported elsewhere.[15] The FIXCIT experiments used two 24 m^3 fluorinated ethylene propylene (FEP) Teflon chambers. One chamber was used for "low NO" experiments (<100 parts-per-trillion (ppt_v)) and the other for "high NO" experiments (NO at parts-per-billion (ppb_v) levels). All experiments were performed at 25 °C except for "slow" OH oxidation experiments in which the temperature was increased to 40 °C. The primary source of OH was either photolysis of H_2O_2 (for low NO conditions) or methyl nitrite (CH_3ONO; for high NO conditions). The concentration of OH was ~10^6 molecules cm^{-3} for all OH oxidation experiments except for experiments where low levels of UV lights were used to generate OH. Ozonolysis experiments were initiated with an ozone-to-isoprene ratio between five and seven. Nitrate radical (NO_3) oxidation was performed in the presence of parts-per-million (ppm_v) levels of formaldehyde (HCHO) to create conditions where the reaction of HO_2 + RO_2 would be competitive with NO_3 + RO_2 and RO_2 + RO_2.[16] NO_3 was generated in the chamber by reacting ~150 ppb_v of NO_2 with ~75 ppb_v of O_3. The relative humidity (RH) in the chamber was ~50% for one OH oxidation and two ozonolysis experiments, otherwise experiments were performed in dry (RH < 5%) air. One OH oxidation experiment included the addition of deliquesced $(NH_4)_2SO_4$ seed aerosol (experiment 19). These experiments are summarized in Table S1.

While we present results from oxidation experiments involving α-pinene or non-OH oxidants, we focus on the results from the OH oxidation experiments of isoprene and isoprene oxidation products. Other experiments where relevant results are presented but not discussed in detail in this manuscript are discussed in the Supporting Information (Section S3).

Instrumentation. This study focuses on gas-phase formic and acetic acid. Two different chemical ionization mass spectrometers employing CF_3O^- as the reagent ion (CF_3O^- CIMS) measured organic acids during FIXCIT; a time-of-flight CIMS measured formic acid, while a triple-quad CIMS detected differentiated isobaric compounds (such as acetic acid and glycolaldehyde) based on their unique fragmentation and ion-clustering patterns.[16−20] The CF_3O^- CIMS were calibrated for the organic acids using neat commercial standards (formic acid, HCOOH, and isotopically labeled acetic acid, $^{13}CH_3{}^{13}COOH$, both Sigma-Aldrich 95−99%) in permeation tubes that were kept at a constant (50 °C) temperature. The sensitivity of formic and acetic acid to chamber relative humidity was corrected with a humidity-dependent calibration curve for each compound.

Chamber Background Subtraction of Organic Acids. Chamber studies demonstrate that formic and acetic acid are gas-phase oxidation products from biogenic precursors, but they also show that these acids have particularly high backgrounds in chamber experiments.[15,21−24] To minimize this background, the Teflon bags were flushed with purified air with the UV lights on to promote oxidation and desorption of material that had deposited on bags during previous experiments. Despite this overnight cleaning procedure, organic acid production was observed during the "blank" experiments in which clean air and oxidant precursors were introduced to the bag and the UV lights turned on. To account for these effects, we consider organic acids produced during the three "blank" experiments as a background that is subtracted for other experiments. For example, most low NO OH experiments were

https://dx.doi.org/10.1021/acsearthspacechem.0c00010
ACS Earth Space Chem. 2020, 4, 730−740

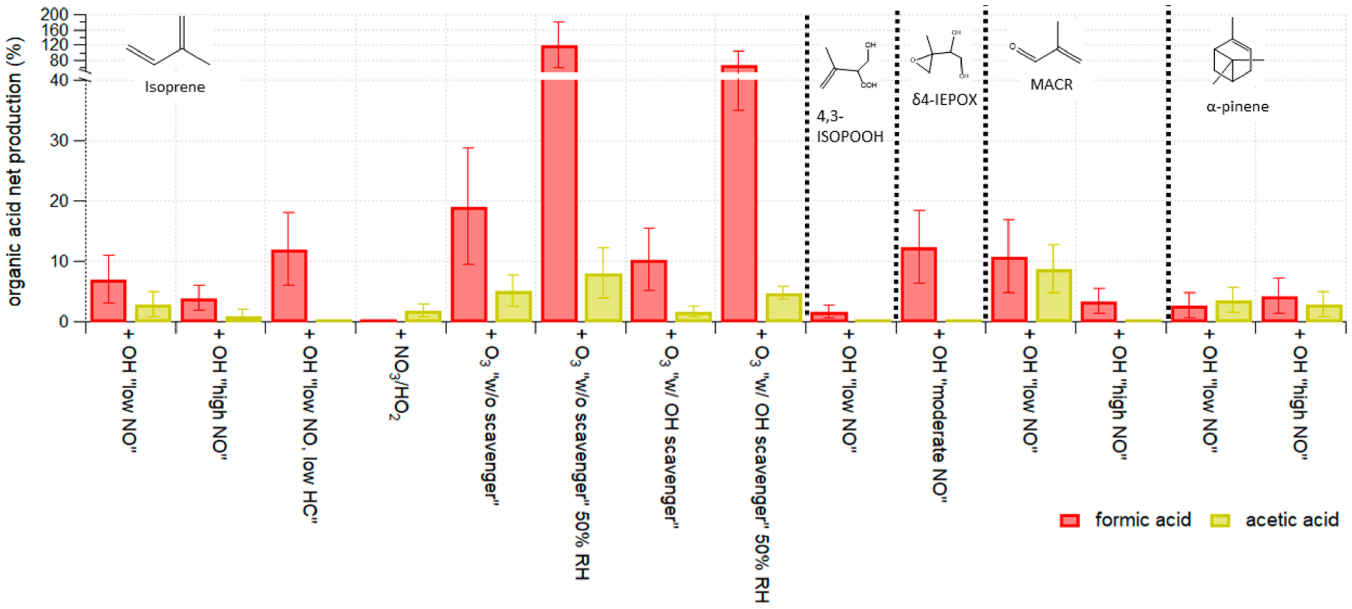

Figure 2. Formic (red bars) and acetic (yellow bars) acid net production (%) are separated by precursor (black dotted lines) and experiment (*x*-axis). Experiments are defined by oxidant, presence of NO, humidity, and/or presence of an OH scavenger. Net production values are derived from a single point at the defined "end" of the experiment (when OH exposure is ~2.2×10^{10} molecules s cm^{-3} or all the precursor is consumed for O_3 and NO_3 oxidation). Errors on the net production are propagated from the uncertainty in the precursor and organic acid background-subtracted measurements.

conducted with all UV lights on and H_2O_2 photolysis as the OH precursor. To apply a background subtraction to the low NO OH experiments for formic acid, we subtract a timeseries of formic acid taken from the low NO blank experiment, normalized to start at the mixing ratio immediately before the UV lights were turned on during the actual experiment of interest (Figure 1). Backgrounds for high NO OH experiments were defined separately for experiments with UV lights at 50% (H_2O_2 OH precursor; Figure S1). We employ a regression-based background estimation method for experiments where low UV light intensity (i.e., 1%; CH_3ONO OH source) was used (i.e., "slow chemistry" experiments 7 and 16; SI Section 2.2; Figure S3).

Experiments with O_3 and NO_3 oxidants were simpler because very little, if any, organic acids were observed when oxidants (and humidified air if applicable) were mixed in the chamber for approximately an hour before introducing the hydrocarbon precursor, indicating negligible influence of chamber artifacts. For these oxidants, we simply subtracted the average organic acid mixing ratio before the precursor was introduced from the organic acid timeseries for the entire experiment.

The magnitude of the background subtraction (Figure 1) highlights the potential importance of photolysis of surface organic films as potential sources of volatile organic acids.[25] For equivalent OH exposures, background mixing ratios measured from the two background experiments ranged from 4 to 5 and 2 to 3 ppb_v of formic and acetic acid, respectively. We qualify the use of background subtraction in this study by recognizing two major limitations: (1) one blank per chamber was performed at the beginning of the study (i.e., January 4th and 5th), while a second blank was performed in one of the chambers later in the study (January 20th); (2) because the blanks were performed early on in the study they may not represent background levels created by deposition of particles and gases on chamber walls in subsequent experiments, and thus backgrounds used here may represent a lower limit. Characterization of chamber background organic acid production using replicate experiments across varied levels of chamber use are essential for future studies.

Propagation of Uncertainty. We report the uncertainty for organic acid net production as the total uncertainty propagated from organic acid mixing ratios measured during the experiments and representative background experiments, and the uncertainty in the hydrocarbon precursor mixing ratio. Table S6 summarizes the calibration uncertainties associated with each of the relevant measurements during FIXCIT. Organic acid mixing ratios are associated with ±50% calibration uncertainty. The measurement uncertainties are substantial, and thus the errors on an individual experiment are large. Systematic calibration uncertainties can be ignored when comparing yields between different experiments, but background uncertainties must still be considered.

OBSERVED ORGANIC ACID PRODUCTION

Because we expect multiple generations of oxidation to occur during the OH-oxidation experiments and organic acids to be produced at multiple points during this oxidation, we define the production of organic acids from these experiments in terms of "net production". We use this terminology in place of the traditional "yield" definition because "net production" captures the production of organic acids from multiple sources ("yield" is sometimes taken in the literature to just describe a single source). Net production overwhelms the <1% of formic and acetic acid that is lost to reaction with OH during a given experiment. We analyzed OH oxidation experiments such that OH exposure ([OH] × experiment time; molecules s cm^{-3}) was comparable between experiments.

We define the net production of organic acids as the ratio of the background-subtracted mixing ratio of organic acid produced in the experiment with respect to the mixing ratio of reacted hydrocarbon precursor ($ppb_v/ppb_v \times 100$). We

https://dx.doi.org/10.1021/acsearthspacechem.0c00010
ACS Earth Space Chem. 2020, 4, 730−740

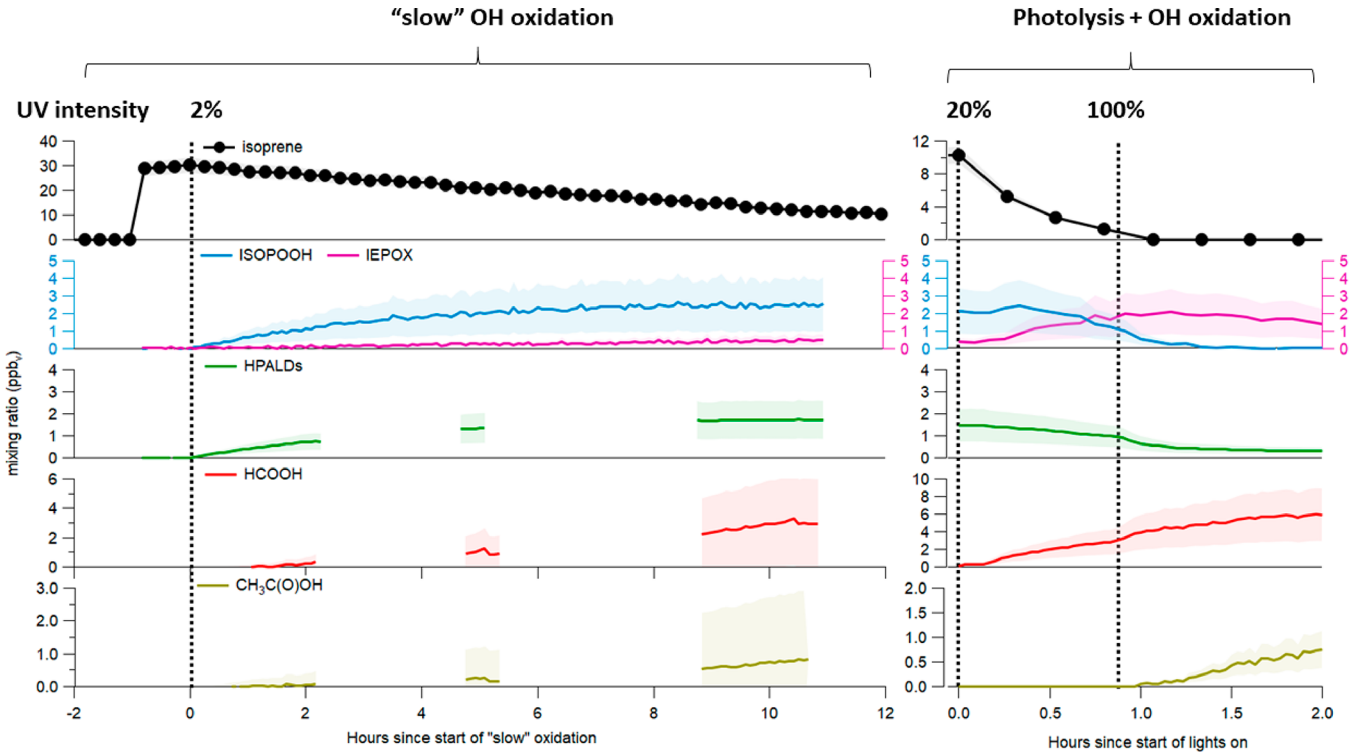

Figure 3. Isoprene (top panels; black trace) was oxidized by OH under conditions of low UV intensity (2% intensity slow oxidation; left panels) to promote the formation of HPALD compounds. High mixing ratios of formic (red trace) and acetic (yellow trace) acids were produced. After the period of slow oxidation, the UV intensity was increased to 20% and then 100% (right panels) to promote photolysis of HPALD compounds. Mixing ratios of organic acids are background subtracted using backgrounds appropriate for the respective UV light conditions. The mixing ratios of acids presented in the panel on the right are shown with contributions from the slow portion of the experiment subtracted out to represent net production from photolysis plus OH oxidation of isoprene oxidation products. Shaded areas represent the uncertainty in the measurements.

report net production for a diverse set of experimental conditions defined by temperature, humidity, oxidant concentration, reaction time, and presence of other trace gases; however, these factors can influence organic acid production by themselves, as evidenced by previous studies.[22,26] We emphasize that net production values calculated from laboratory experiments, such as ours, should be interpreted within the constraints of experimental conditions.

OH Oxidation (Experiments 2, 3, 10, 11, and 21). Oxidation by OH is the dominant daytime sink for both isoprene ($\tau_{OH} \approx 2$ h; 298 K; [OH] = 1.5×10^6 molecules cm^{-3}) and α-pinene ($\tau_{OH} \approx 3-4$ h; 298 K; [OH] = 1.5×10^6 molecules cm^{-3}). Several of the oxidation products from isoprene also have lifetimes with respect to OH oxidation on the order of hours, and we thus expect multiple generations of oxidation products to occur during the multiple hour-long chamber experiments. Peroxy radicals (ISOPOO) form upon OH oxidation of isoprene, and subsequent oxidation products are determined through specific bi- and unimolecular RO_2 reaction pathways. OH experiments encompassed a range of NO/HO_2 ratios to control the fate of RO_2.

NO clearly influences organic acid yields from isoprene oxidation (Figure 2). In the isoprene low NO experiments (i.e., NO/HO_2 ratio <0.5), HO_2 preferentially reacts with RO_2 to form characteristic products like isoprene hydroxy hydroperoxides (ISOPOOH) and isoprene epoxydiols (IEPOX). For reference, at NO/HO_2 ratios of ~1 the rate of RO_2 reaction with HO_2 should be approximately twice as fast as with NO. Three of the experiments (OH oxidation of IEPOX and slow OH oxidation of isoprene and α-pinene) were performed under conditions of "moderate NO" with NO/HO_2 ratios of 2−4. Under these conditions, NO reaction with RO_2 may be equal or slightly more competitive than with HO_2, though this depends on the structure of the RO_2. For experiments where NO/HO_2 was >100 (high NO), the fate of RO_2 is determined almost exclusively through reaction with NO. In the case of isoprene-derived RO_2, H-shift isomerization reactions compete with RO_2 bimolecular reactions.

Increasing NO suppresses organic acid yields during OH oxidation of isoprene, suggesting that the RO_2 reaction pathways involving HO_2, RO_2, or H-shift isomerization dominantly produce organic acids. This observation is consistent with the findings of Paulot et al.[27] MACR oxidation is similar with higher formic acid yields under low NO than high NO conditions, and no acetic acid produced during high NO experiments. The low NO oxidation of 4,3-ISOPOOH produced a factor of 4 lower formic acid yields than the low NO isoprene oxidation experiment, suggesting that first generation isoprene products other than 4,3-ISOPOOH are the precursors for organic acids. There are two ISOPOOH isomers, and the major isomer (1,2-ISOPOOH) may still be a substantial organic acid precursor, although 4,3-ISOPOOH is clearly not. Other first-generation products from isoprene + OH chemistry include hydroperoxy enals (HPALDs) from the isomerization pathway or products from RO_2 self-termination reactions.

In contrast to isoprene, α-pinene does not show a substantial influence of NO on organic acid yields. However, organic acid production from OH oxidation of α-pinene is relatively low

https://dx.doi.org/10.1021/acsearthspacechem.0c00010
ACS Earth Space Chem. 2020, 4, 730−740

compared to isoprene, and we focus on isoprene sources of formic and acetic acids.

One intriguing pair of experiments subjected two different isoprene concentrations (42 vs 21 ppb_v) to otherwise identical low NO OH oxidation (i.e., identical amounts of OH exposure). Decreasing the hydrocarbon precursor concentrations increased the lifetime of RO_2 with respect to self-termination reactions. RO_2 termination pathways should thus be more influenced by reaction with HO_2 or isomerization pathways than RO_2 self-reaction. The experiment with half the isoprene precursor resulted in double the formic acid yield (i.e., 15% vs 7%). On the other hand, acetic acid was not produced in levels that exceeded background concentrations in the experiment with the lower amount of isoprene precursor. These observations suggest that RO_2 + RO_2 are not sources of formic acid but are instead sources of acetic acid.

Slow OH Oxidation (Experiments 7 and 16). When RO_2 bimolecular lifetimes are long (~100 s), recent studies have determined that first-generation isoprene OH-adduct RO_2 (i.e., ISOPOO) can react through isomerization to produce isoprene hydroperoxy enals (HPALDs; $C_5H_8O_3$; yield = 25−75%) at a rate competitive with bimolecular reactions.[9,28,29] Extending RO_2 lifetimes in chamber studies to reach this regime is challenging.[15,30] Because of the reversible nature of O_2 addition to form ISOPOO, extending the ISOPOO lifetime likely brings this RO_2 population closer to the equilibrium distribution, thereby producing compounds more relevant to pristine ambient environments.[31]

Long RO_2 lifetimes were achieved during FIXCIT using very low levels of OH, NO, and HO_2 radicals for OH oxidation of isoprene (the "slow, moderate NO" experiment). The yields of formic (17.5%) and acetic (4.3%) acids were much higher in this experiment compared to the standard low NO experiment (Figures 3, S4). This highlights the importance of isomerization in isoprene oxidation and the subsequent production of organic acids. This result is consistent with observations of high concentrations of organic acids in forest environments with low anthropogenic influence, where RO_2 isomerization is considered important.[9,12,13]

Unimolecular processes representative of slow chemistry are poorly understood for monoterpenes compared to isoprene. Isomerization of monoterpene-derived RO_2 has been determined to be competitive with bimolecular reactions based on observations of highly oxidized molecules formed from autoxidation.[32,33] The rates of these reactions, however, have not been well quantified.[28,34] Xu et al.[35] recently measured the isomerization rate of first-generation RO_2 resulting from the 4-member ring-opening of α-pinene to be $4 \pm 2\ s^{-1}$, suggesting that these processes are competitive or faster than other monoterpene-derived RO_2 fates. In one experiment, we oxidized α-pinene with OH under low UV light to extend RO_2 lifetimes and explore the effects of isomerization on RO_2 termination ("slow, moderate NO α-pinene"). Here, we also observed high yields of formic (14.5%) and acetic (5.5%) acid (Figure S4). Isomerization of α-pinene RO_2 could be an important source of organic acids in monoterpene-dominated environments although further experiments with careful background subtraction are essential.

Oxidation through Photolysis (Experiments 7 and 16). HPALDs and dihydroperoxy carbonyls (DHP) are potentially important sources of formic acid in the low NO and slow isoprene oxidation experiments. These oxidation products are formed from the 1,6-H shift isomerization of Z-δ-ISOPOO. If formed in substantial yield, then decomposition, photolysis or OH-reaction of these isomerization products could be a source of organic acids. The rates of HPALD formation are uncertain due to the strong temperature dependences in both the 1,6-H shift and the equilibrium between allylic radicals and ISOPOO and the differing propensity for isoprene to form HPALDs depending on whether OH addition occurs at C1 or C4.[36] Additionally, several other compounds have been observed from the isomerization of ISOPOO in addition to HPALDs.[29,37]

After ~1.5 ppb_v of HPALDs were formed in the slow isoprene experiment, the UV intensity was increased, and combined photolysis and OH reaction of the resulting HPALD compounds occurred over the course of 2 h (OH exposure ~3×10^{10} molecules s cm^{-3}). Despite the OH exposure being a little less than half of the exposure determined for the standard low NO experiment, combined photolysis and OH reaction of HPALDs, and associated compounds produced high mixing ratios of formic and, albeit to a lesser extent, acetic acid (Figure 3) in this HPALD photoxidation experiment. While 10 ppb_v of isoprene was still present when the UV lights were turned on to high intensity, this isoprene is likely only a minor source of formic acid from the HPALD + photolysis experiment. Photolysis and OH reaction of HPALDS and compounds produced from the ISOPOO H-shift isomerization pathway thus contribute to formic acid production. However, oxidation of organic films on chamber walls is a likely source of persistent formic and acetic acid backgrounds and we speculate that this chemistry spuriously enhances observed formic acid production in this experiment. Accounting for this surface film oxidation is challenging but must be accounted for in future experiments.

Consistent with the isoprene oxidation experiments, high mixing ratios of organic acids were also observed from the combined photolysis and OH oxidation of slow chemistry products from α-pinene (Figure S5), and isomerization products from α-pinene OH oxidation are potentially important precursors of organic acids. In the ambient atmosphere, where isomerization processes are competitive with bimolecular RO_2 fates, daytime oxidation of monoterpene isomerization products may be a source of organic acids.

■ MISSING SOURCES OF ORGANIC ACIDS

The chamber experiments enable identification of specific points in the isoprene oxidation mechanism where organic acids must be produced in significant quantities. In particular, we focus on MACR, ISOPOOH, and IEPOX oxidation by OH to elucidate organic acid production from these oxidation products of isoprene.

We investigate organic acid formation chemistry using the Framework for 0D Atmospheric Modeling (F0AM) v3.1[38] (MATLAB R2018b) equipped with the following three different isoprene oxidation mechanisms: (1) the Master Chemical Mechanism v3.3.1 (MCM),[39] (2) the Wennberg Reduced+ semiexplicit mechanism (WR+),[36] and (3) the Model of Atmospheric composition at Global and Regional scales using Inversion Techniques for Trace gas Emissions (MAGRITTE v1.1).[9] This setup allows us to test the sensitivity of organic acid production to mechanistic differences in isoprene oxidation. MCM is a near-explicit, comprehensive mechanism that is based on Jenkin et al.[39] and contains 610 species and 1974 reactions. Importantly, when representing peroxy radical self-termination pathways,

https://dx.doi.org/10.1021/acsearthspacechem.0c00010
ACS Earth Space Chem. 2020, 4, 730−740

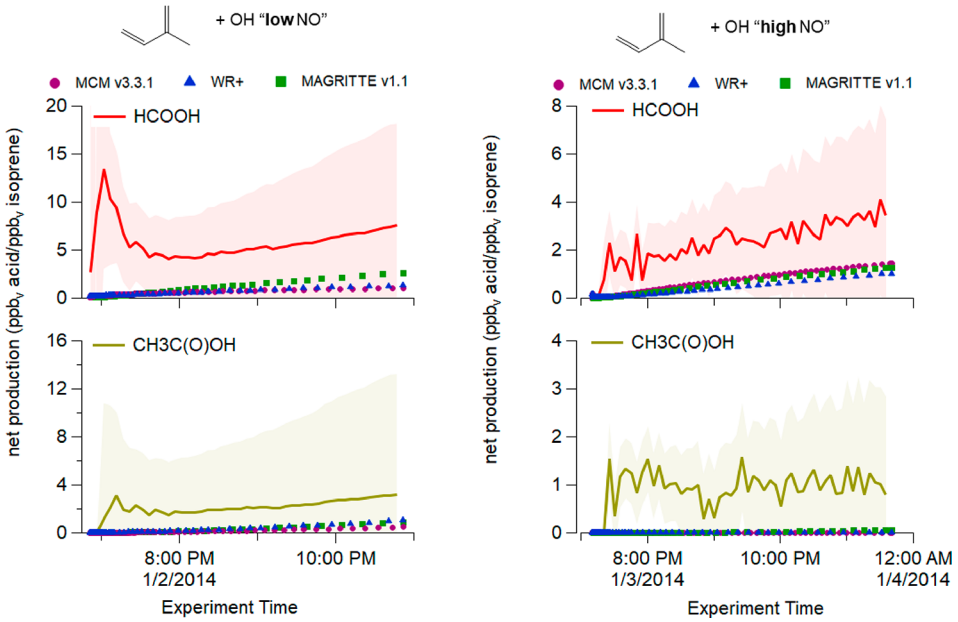

Figure 4. Measured production (solid lines) of formic (red) and acetic (yellow) acids for the isoprene + OH experiments performed under conditions of low NO (left) and high NO (right). Model predictions from each of the three isoprene oxidation mechanisms, modified to include estimated yields of acids from other FIXCIT experiments, are shown by markers. Shaded regions represent propagated uncertainty in production of organic acids.

MCM groups all RO_2 as a single species that reacts indiscriminately with other unique RO_2. Wennberg et al.[36] summarized theoretical and laboratory work on isoprene oxidation into the WR+ mechanism.[28] The WR+ mechanism contains 155 species and 429 reactions and builds upon the mechanistic architecture presented in the MCM by modifying RO_2 + NO branching ratios, updating H-shift isomerization reactions, and explicitly including reaction products with ≥1% overall yield from isoprene. The MAGRITTE mechanism builds upon the Leuven Isoprene Mechanism, the Wennberg mechanism, and the MCM. Unique features of MAGRITTE include incorporation of findings from recent laboratory work analyzing OH-oxidation of isoprene under conditions of low NO and HO_2 mixing ratios,[29] photolysis of hydroperoxycarbonyls to produce enols and keto-enols that rapidly react with OH,[40,41] and a reassessment of the influence of stabilized Criegee intermediates (sCI) in the formation of formic acid.[18,42]

We modeled FIXCIT experiments by modifying the "base case" mechanisms to account for likely important sources of formic and acetic acid. These modifications include addition of the reaction of HCHO + HO_2 that forms formic acid,[43] updates to the quantum yield for the photoautomerization of acetaldehyde to vinyl alcohol,[44] and inclusion of OH oxidation of vinyl alcohol to formic acid with a 14% yield.[45] We follow the findings of Assaf et al.,[46] who determined the reaction of OH with CH_3O_2 produced a Criegee intermediate with <5% yield, and exclude this reaction as a source of formic acid.[47] Base case simulations for the FIXCIT isoprene oxidation experiments predicted organic acid yields orders of magnitude lower than observed (Table S2). We increased organic acid yields on specific RO_2 reactions to improve organic acid model-measurement agreement, first working with MACR, then IEPOX, then ISOPOOH. Specific modifications to each mechanism are provided in Table S3. We do not retain carbon-balance when applying modifications to the mechanisms, so the yields only test the sensitivity of organic acid production to specific pathways.

Below we describe how modifications to the model impact formic and acetic acid from isoprene + OH oxidation.

Isoprene + OH. Here we apply the modified isoprene oxidation mechanisms to two experiments of OH + isoprene performed under conditions of "low" and high NO (experiments 2 and 3, respectively).

Isoprene + OH low NO. The primary fate (>90%) of ISOPOO in the isoprene + OH low NO experiment was reaction with HO_2 and formed ISOPOOH as a major product. Subsequent reactions of isoprene oxidation products in the low NO environment promote the formation of multifunctional compounds, such as peroxy or hydroxy carbonyls, that are reactive toward OH or susceptible to photolysis. During FIXCIT, the low NO OH-oxidation experiments produced higher yields of organic acids from isoprene oxidation compared to the high NO pathways.

All three mechanisms predict similar (within 50%) formic and acetic acid mixing ratios from the isoprene + OH low NO experiment (Figure 4; Table S2). MAGRITTE predictions are closest to the observation. More than 50% of the formic acid predicted in all mechanisms comes from the modified yields to MACR and ISOPOOH informed by the FIXCIT experiments. The rest of the formic acid predicted from WR+ and the MCM comes from chemistry involving sCIs. In contrast, the MAGRITTE mechanism is informed by work that does not support a high direct yield of formic acid from the reaction of sCIs with water and thus predicts low contributions of formic acid from this pathway.[42] MAGRITTE does, however, predict significant yields (20% for 4,1-ISOPOOH and 32% for 4,3-ISOPOOH) of formic acid from photolysis and OH oxidation of products formed from the H-abstraction channel of ISOPOOH OH oxidation. All the mechanisms predict that more than 50% of the acetic acid produced comes from the termination of the CH_3CO_3 radical by HO_2 with significant

https://dx.doi.org/10.1021/acsearthspacechem.0c00010
ACS Earth Space Chem. 2020, 4, 730−740

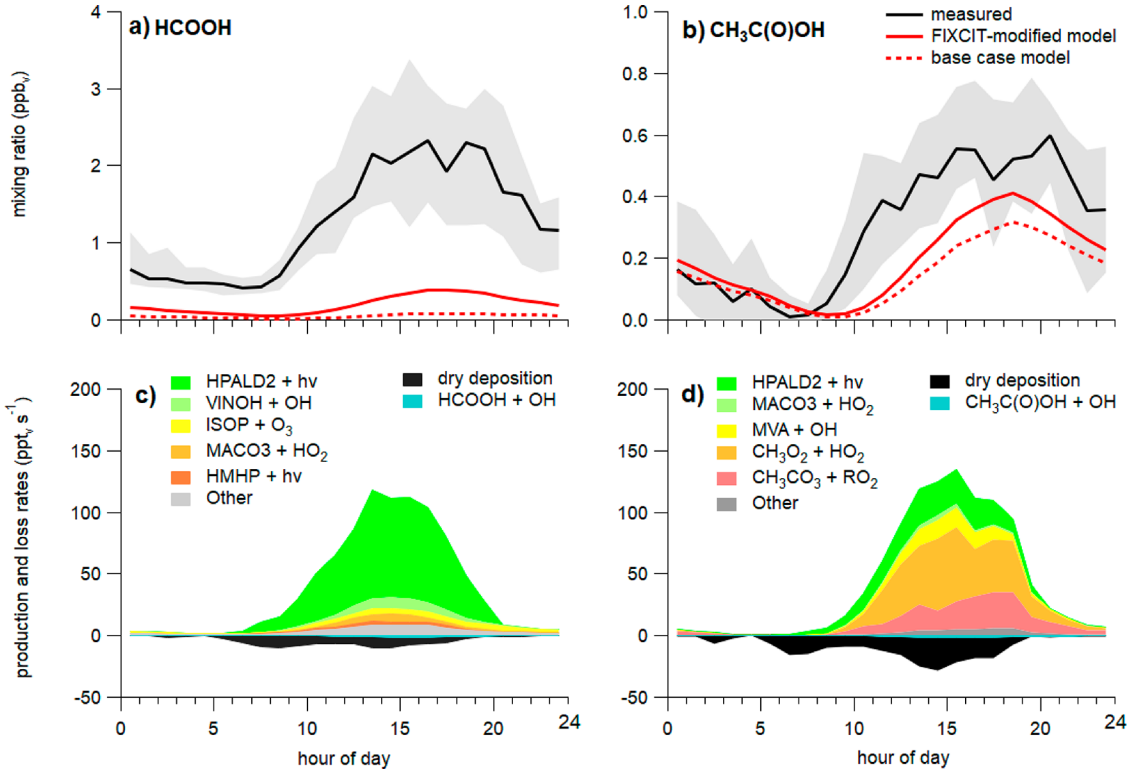

Figure 5. Formic (a) and acetic (b) acid mixing ratio measured (black line; average diel profile), predicted from MAGRITTE (red dashed line), and predicted from FIXCIT (red solid line; modified MAGRITTE) during SOAS. Shaded regions represent the 25th and 75th percentiles. Modeled rates of production and loss for formic (c) and acetic (d) acid are separated by reaction.

contributions from the termination of the RO_2, produced from abstraction of the aldehydic hydrogen on MACR (MACO3 in MCM v3.3.1), by HO_2. The MAGRITTE mechanism predicts more acetic acid than the other two mechanisms because of the inclusion of reactions that form methyl vinyl alcohol that reacts with OH to form acetic acid.

Few studies have looked at formic or acetic acid production from OH oxidation of isoprene, and no literature values are available for yields of acids from isoprene oxidation products such as methyl vinyl ketone. To close the gap between measurement and model predictions, we apply a yield of formic acid to the photolysis of the HPALD compounds. High yields of both formic and acetic acid were observed during the slow chemistry photolysis experiment. HPALD photolysis yields are only applied to investigate the model-measurement gap for formic acid in the isoprene + OH low NO experiment (These yields are unrealistically high and produce three moles of formic acid per mole of HPALD photolyzed; Table S3).

Isoprene + OH high NO. In the isoprene + OH high NO experiment, the ISOPOO fate was dominated by reaction with NO. Major products from this reaction include isoprene hydroxy nitrates, unsaturated isoprene hydroxy carbonyls, MACR, and MVK. However, Peeters et al.[48] note that the population of ISOPOO produced in chamber experiments is kinetically determined by the decrease in the bimolecular lifetime of ISOPOO as a result of very high levels of NO in the experiments. Accordingly, product yields are very sensitive to the ISOPOO isomer distribution, which complicates interpretation from chamber experiments.

The yields of formic and acetic acid from the high NO oxidation of isoprene were approximately half that of the low NO oxidation experiment. All the mechanisms predict ~50% of the experimentally observed formic acid production but only predict <5% of the experimentally observed acetic acid production in the high NO experiment (Figure 4; Table S2). The WR+ predicts significant formic acid production from OH oxidation of an MVK hydroxy nitrate, and all the mechanisms predict only minor contributions from reaction of the first-generation IEPOX RO_2 by NO. MAGRITTE predicted the highest levels of acetic acid because of its unique reaction of methyl vinyl alcohol with OH.

Paulot et al.[16] observed higher yields of formic (10%) and acetic (3%) acid than FIXCIT. However, Paulot et al. did not consider oxidation of deposited organic vapors on the chamber wall, and those yields agree well with our pre- background subtraction yields. Paulot et al. attributed most observed formic acid to decomposition of first-generation isoprene hydroxy nitrate (ISOPN) and OH oxidation of glycolaldehyde. 4,3-ISOPN was oxidized with OH during FIXCIT, but that experiment does not provide evidence for an isoprene nitrate source of formic acid. Our model results showed only small (<5%) contributions from glycoaldehyde to formic acid production. Also in contrast to Paulot et al, but consistent with Butkovskaya et al.,[49] the FIXCIT experiments do not support hydroxyacetone as a major source of acetic acid in the OH oxidation of isoprene under high NO conditions: acetic acid did not exceed background in the MACR + OH high NO experiment. When we included hydroxyacetone as an acetic acid source, our model overpredicted acetic acid production.

SOURCES OF FORMIC AND ACETIC ACID DURING SOAS

We simulate organic acids during SOAS using the modified MAGRITTE mechanism with yields determined above from

https://dx.doi.org/10.1021/acsearthspacechem.0c00010
ACS Earth Space Chem. 2020, 4, 730−740

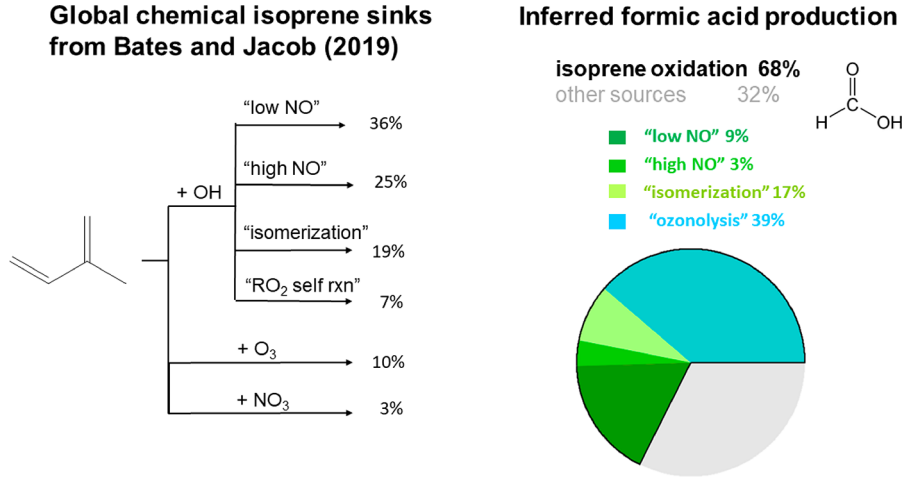

Figure 6. Global isoprene chemical sinks as determined by Bates and Jacob,[51] and our estimated contribution of isoprene oxidation to global formic acid production. The black outline of the pie chart shows the fraction of global formic acid production resulting from isoprene oxidation (68%). Applying the FIXCIT results to the chemical isoprene sinks determines the relative contribution from ozonolysis and low NO, high NO, and "isomerization" pathways of isoprene oxidation by OH.

the FIXCIT experiments. We use the MAGRITTE mechanism here because of its specific consideration of OH oxidation of enols. The model includes the dry deposition scheme developed in Nguyen et al.[14] for oxidized organic compounds. Following Kaiser et al.,[50] the model constrains a suite of VOCs and inorganic trace gases to measured median diel profiles from the campaign (Table S4). If absent from MAGRITTE, VOC reactions followed the MCM v3.3.1. Further details of the ambient simulation are in Section 7 of the Supporting Information.

Modeled formic and acetic acid mixing ratios (see Figure 5) are generally underpredicted by 85% and 35%, respectively. The modeled temporal distribution of formic acid is reasonably represented by the model (r^2 = 0.82), but the rapid morning increase in both organic acid mixing ratios is not. However, we acknowledge that this model does not include known minor formic acid sources such as soil and plant emissions, contributions from mixing of entrained air, nor does it consider advection from other regions. Further, the model considers few monoterpene oxidation sources. The underprediction of acetic acid was much smaller than formic acid, suggesting that many of the most important gas-phase production reactions are well-represented in the chemical mechanism used here. In contrast to acetic acid, significant sources of formic acid are still missing, even with the additions noted above. For both acids, the major model sink is dry deposition. However, if additional source mechanisms are added to match the observations, additional sink terms may be required to maintain the diel profiles.

Most of the acetic acid production is from reactions of CH_3CO_3 radicals with HO_2 and RO_2. Approximately 25% of the production originates from other sources, such as the MACO3 + HO_2 reaction modified with a yield determined from the MACR + OH low NO FIXCIT experiment.

According to the model, the dominant formic acid source is HPALD photolysis. However, this source was added to the mechanism to force model predictions of formic acid to agree with measurements during the isoprene + OH low NO FIXCIT experiment, although this source is only loosely supported by the slow chemistry photolysis experiment. Other important sources include vinyl alcohol (produced from phototautomerization of acetaldehyde) oxidation, isoprene ozonolysis (yield determined from FIXCIT experiments, Figure 2), and MACO3 + HO_2 (yield determined from the MACR + OH low NO FIXCIT experiment).

IMPLICATIONS FOR GLOBAL FORMIC ACID

Despite recent updates to isoprene oxidation mechanisms, global simulations continue to underestimate ambient levels of formic and acetic acid (see Figure 6).[3,9,51] The high yields of formic and acetic acid measured during the FIXCIT experiments suggest isoprene oxidation is a major atmospheric source of these acids. A GEOS-Chem simulation of the global chemical sinks of isoprene quantified the fate of ISOPOO.[51] Applying the FIXCIT yields from Figure 2 to the reported isoprene chemical sink distribution provides a global annual production rate of 74 Tg a^{-1} of formic acid and 15 Tg a^{-1} of acetic acid (Table S5). This estimated acetic acid source is similar to other studies, but this estimated formic acid source is ~3× higher than previous studies. Major contributors to our estimate are isoprene ozonolysis (~55%) and ISOPOO isomerization (~24%). Our estimated global formic acid production still falls below the satellite-constrained values of 100−120 Tg a^{-1}.[3] On the basis of the substantial background formic acid in the FIXCIT chamber experiments, we hypothesize that multiphase chemistry of organic films on aerosols or biosphere surfaces may account for a substantial fraction of the missing global organic acid source. While our estimate does not consider the complexities inherent in global modeling or uncertainties in our results, it does highlight the potential importance of isoprene oxidation as a global source of formic acid.

Despite modifications to the chemical mechanisms, the model-measurement discrepancy in formic acid at SOAS persists. In contrast, the model captures ambient acetic acid within a factor of 2. The FIXCIT experiments highlighted the importance of experimental conditions in which RO_2 lifetimes are similar to the atmosphere (i.e., slow OH oxidation experiments). These slow experiments suggested that compounds associated with the 1,6-H shift isomerization reactions of ISOPOO, such as HPALDs or DHPs, are potentially important sources of formic acid. FIXCIT also demonstrated

https://dx.doi.org/10.1021/acsearthspacechem.0c00010
ACS Earth Space Chem. 2020, 4, 730−740

that NO termination reactions can suppress formation of organic acids.

The biggest challenge we faced assessing the experimental and atmospheric relevance of our results was the substantial "background" production of formic and acetic acids in the absence of injected VOC. This substantial organic acid production is likely due to oxidation of organic films deposited on the chamber walls. Wall loss is reversible for some gases and occurs simultaneously with gas-phase VOC oxidation and is thus challenging to robustly quantify without careful, frequent blank experiments. However, the high formic acid backgrounds observed during chamber experiments highlight the potential for surface chemistry sources of these acids. Oxidation of organic molecules on ecosystem and aerosol surfaces may thus be a relevant formic acid source in the ambient atmosphere.

■ ASSOCIATED CONTENT

Supporting Information

The Supporting Information is available free of charge at https://pubs.acs.org/doi/10.1021/acsearthspacechem.0c00010.

Details of the FIXCIT experiments, further discussions and examples of background subtraction methods, and analyses of other oxidation experiments (i.e., ozonolysis and slow OH oxidation) that contributed to the results; details of the box modeling and global formic acid production calculations (PDF)

■ AUTHOR INFORMATION

Corresponding Author

Delphine K. Farmer − *Department of Chemistry, Colorado State University, Fort Collins, Colorado 80523, United States;* orcid.org/0000-0002-6470-9970; Email: Delphine.Farmer@colostate.edu

Authors

Michael F. Link − *Department of Chemistry, Colorado State University, Fort Collins, Colorado 80523, United States;* orcid.org/0000-0002-1841-2455

Tran B. Nguyen − *Department of Environmental Toxicology, University of California Davis, Davis, California 95616, United States*

Kelvin Bates − *Paulson School of Engineering and Applied Sciences, Harvard University, Cambridge, Massachusetts 02138, United States;* orcid.org/0000-0001-7544-9580

Jean-François Müller − *Royal Belgian Institute for Space Aeronomy, 1180 Brussels, Belgium*

Complete contact information is available at: https://pubs.acs.org/10.1021/acsearthspacechem.0c00010

Funding

We acknowledge the National Science Foundation (AGS 1240611) and the Arnold and Mabel Beckman Foundation (Young Investigator Award) for funding this work. FIXCIT was made possible by the support from multiple agencies: the U.S. National Science Foundation (NSF) under Grants AGS-1240604 (Caltech), AGS-1246918 (Penn State University), AGS-1247421 (UWM), AGS-1243354 (Colorado Univerisity), and AGS-1120076 (UC-Berkeley); the U.S. Department of Energy under Grant DE-SC0006626 (Caltech); and the U.S. Environmental Protection Agency (EPA) under STAR Grant 835407 (PNNL/UCB/SUNY).

Notes

The authors declare no competing financial interest.

■ ACKNOWLEDGMENTS

We thank Glenn Wolfe for help with F0AM. We would also like to acknowledge John Crounse, Jason St. Clair, and Paul Wennberg for help with measurements and useful feedback from the FIXCIT experiments.

■ REFERENCES

(1) Millet, D. B. Atmospheric Chemistry: Natural Atmospheric Acidity. *Nat. Geosci.* **2012**, *5* (1), 8−9.

(2) Metzger, S.; Mihalopoulos, N.; Lelieveld, J. Importance of Mineral Cations and Organics in Gas-Aerosol Partitioning of Reactive Nitrogen Compounds: Case Study Based on MINOS Results. *Atmos. Chem. Phys.* **2006**, *6* (9), 2549−2567.

(3) Stavrakou, T.; Müller, J.-F.; Peeters, J.; Razavi, A.; Clarisse, L.; Clerbaux, C.; Coheur, P.-F.; Hurtmans, D.; De Mazière, M.; Vigouroux, C.; et al. Satellite Evidence for a Large Source of Formic Acid from Boreal and Tropical Forests. *Nat. Geosci.* **2012**, *5* (1), 26−30.

(4) Bannan, T. J.; Murray Booth, A.; Le Breton, M.; Bacak, A.; Muller, J. B. A.; Leather, K. E.; Khan, M. A. H.; Lee, J. D.; Dunmore, R. E.; Hopkins, J. R. Seasonality of Formic Acid (HCOOH) in London during the ClearfLo Campaign. *J. Geophys. Res. Atmospheres* **2017**, *122* (22), 12488−12498.

(5) Paulot, F.; Wunch, D.; Crounse, J. D.; Toon, G. C.; Millet, D. B.; DeCarlo, P. F.; Vigouroux, C.; Deutscher, N. M.; González Abad, G.; Notholt, J.; et al. Importance of Secondary Sources in the Atmospheric Budgets of Formic and Acetic Acids. *Atmos. Chem. Phys.* **2011**, *11* (5), 1989−2013.

(6) Chaliyakunnel, S.; Millet, D. B.; Wells, K. C.; Cady-Pereira, K. E.; Shephard, M. W. A Large Underestimate of Formic Acid from Tropical Fires: Constraints from Space-Borne Measurements. *Environ. Sci. Technol.* **2016**, *50* (11), 5631−5640.

(7) Millet, D. B.; Baasandorj, M.; Farmer, D. K.; Thornton, J. A.; Baumann, K.; Brophy, P.; Chaliyakunnel, S.; de Gouw, J. A.; Graus, M.; Hu, L.; et al. A Large and Ubiquitous Source of Atmospheric Formic Acid. *Atmos. Chem. Phys.* **2015**, *15* (11), 6283−6304.

(8) Chen, X.; Millet, D. B.; Singh, H. B.; Wisthaler, A.; Apel, E. C.; Atlas, E. L.; Blake, D. R.; Bourgeois, I.; Brown, S. S.; Crounse, J. D.; et al. On the Sources and Sinks of Atmospheric VOCs: An Integrated Analysis of Recent Aircraft Campaigns over North America. *Atmos. Chem. Phys.* **2019**, *19* (14), 9097−9123.

(9) Müller, J.-F.; Stavrakou, T.; Peeters, J. Chemistry and Deposition in the Model of Atmospheric Composition at Global and Regional Scales Using Inversion Techniques for Trace Gas Emissions (MAGRITTE v1.1) − Part 1: Chemical Mechanism. *Geosci. Model Dev.* **2019**, *12* (6), 2307−2356.

(10) Schobesberger, S.; Lopez-Hilfiker, F. D.; Taipale, D.; Millet, D. B.; D'Ambro, E. L.; Rantala, P.; Mammarella, I.; Zhou, P.; Wolfe, G. M.; Lee, B. H.; et al. High Upward Fluxes of Formic Acid from a Boreal Forest Canopy. *Geophys. Res. Lett.* **2016**, *43* (17), 9342−9351.

(11) Fulgham, S. R.; Brophy, P.; Link, M.; Ortega, J.; Pollack, I.; Farmer, D. K. Seasonal Flux Measurements over a Colorado Pine Forest Demonstrate a Persistent Source of Organic Acids. *ACS Earth Space Chem.* **2019**, *3*, 2017−2032.

(12) Alwe, H. D.; Millet, D. B.; Chen, X.; Raff, J. D.; Payne, Z. C.; Fledderman, K. Oxidation of Volatile Organic Compounds as the Major Source of Formic Acid in a Mixed Forest Canopy. *Geophys. Res. Lett.* **2019**, *46* (5), 2940−2948.

(13) Brophy, P.; Farmer, D. K. A Switchable Reagent Ion High Resolution Time-of-Flight Chemical Ionization Mass Spectrometer for Real-Time Measurement of Gas Phase Oxidized Species: Characterization from the 2013 Southern Oxidant and Aerosol Study. *Atmos. Meas. Tech.* **2015**, *8* (7), 2945−2959.

(14) Nguyen, T. B.; Crounse, J. D.; Teng, A. P.; Clair, J. M. S.; Paulot, F.; Wolfe, G. M.; Wennberg, P. O. Rapid Deposition of

Oxidized Biogenic Compounds to a Temperate Forest. *Proc. Natl. Acad. Sci. U. S. A.* **2015**, *112* (5), E392−E401.
(15) Nguyen, T. B.; Crounse, J. D.; Schwantes, R. H.; Teng, A. P.; Bates, K. H.; Zhang, X., St.; Clair, J. M.; Brune, W. H.; Tyndall, G. S.; Keutsch, F. N.; et al. Overview of the Focused Isoprene eXperiment at the California Institute of Technology (FIXCIT): Mechanistic Chamber Studies on the Oxidation of Biogenic Compounds. *Atmos Chem. Phys.* **2014**, *14* (24), 13531−13549.
(16) Paulot, F.; Crounse, J. D.; Kjaergaard, H. G.; Kroll, J. H.; Seinfeld, J. H.; Wennberg, P. O. Isoprene Photooxidation: New Insights into the Production of Acids and Organic Nitrates. *Atmos. Chem. Phys.* **2009**, *9* (4), 1479−1501.
(17) St. Clair, J. M.; McCabe, D. C.; Crounse, J. D.; Steiner, U.; Wennberg, P. O. Chemical Ionization Tandem Mass Spectrometer for the in Situ Measurement of Methyl Hydrogen Peroxide. *Rev. Sci. Instrum.* **2010**, *81* (9), 94102.
(18) Allen, H. M.; Crounse, J. D.; Bates, K. H.; Teng, A. P.; Krawiec-Thayer, M. P.; Rivera-Rios, J. C.; Keutsch, F. N.; St. Clair, J. M.; Hanisco, T. F.; Møller, K. H.; et al. Kinetics and Product Yields of the OH Initiated Oxidation of Hydroxymethyl Hydroperoxide. *J. Phys. Chem. A* **2018**, *122* (30), 6292−6302.
(19) Rivera-Rios, J. C.; Nguyen, T. B.; Crounse, J. D.; Jud, W.; St. Clair, J. M.; Mikoviny, T.; Gilman, J. B.; Lerner, B. M.; Kaiser, J. B.; de Gouw, J.; et al. Conversion of Hydroperoxides to Carbonyls in Field and Laboratory Instrumentation: Observational Bias in Diagnosing Pristine versus Anthropogenically Controlled Atmospheric Chemistry. *Geophys. Res. Lett.* **2014**, *41* (23), 8645−8651.
(20) Clair, J. M. S.; Spencer, K. M.; Beaver, M. R.; Crounse, J. D.; Paulot, F.; Wennberg, P. O. Quantification of Hydroxyacetone and Glycolaldehyde Using Chemical Ionization Mass Spectrometry. *Atmos. Chem. Phys.* **2014**, *14* (8), 4251−4262.
(21) Bates, K. H.; Crounse, J. D.; St. Clair, J. M.; Bennett, N. B.; Nguyen, T. B.; Seinfeld, J. H.; Stoltz, B. M.; Wennberg, P. O. Gas Phase Production and Loss of Isoprene Epoxydiols. *J. Phys. Chem. A* **2014**, *118* (7), 1237−1246.
(22) Friedman, B.; Farmer, D. K. SOA and Gas Phase Organic Acid Yields from the Sequential Photooxidation of Seven Monoterpenes. *Atmos. Environ.* **2018**, *187*, 335−345.
(23) Reed Harris, A. E.; Cazaunau, M.; Gratien, A.; Pangui, E.; Doussin, J.-F.; Vaida, V. Atmospheric Simulation Chamber Studies of the Gas-Phase Photolysis of Pyruvic Acid. *J. Phys. Chem. A* **2017**, *121* (44), 8348−8358.
(24) Schnitzhofer, R.; Metzger, A.; Breitenlechner, M.; Jud, W.; Heinritzi, M.; De Menezes, L.-P.; Duplissy, J.; Guida, R.; Haider, S.; Kirkby, J.; et al. Characterisation of Organic Contaminants in the CLOUD Chamber at CERN. *Atmos. Meas. Tech.* **2014**, *7* (7), 2159−2168.
(25) Malecha, K. T.; Nizkorodov, S. A. Photodegradation of Secondary Organic Aerosol Particles as a Source of Small, Oxygenated Volatile Organic Compounds. *Environ. Sci. Technol.* **2016**, *50*, 9990−9997.
(26) Friedman, B.; Brophy, P.; Brune, W. H.; Farmer, D. K. Anthropogenic Sulfur Perturbations on Biogenic Oxidation: SO2 Additions Impact Gas-Phase OH Oxidation Products of α- and β-Pinene. *Environ. Sci. Technol.* **2016**, *50* (3), 1269−1279.
(27) Paulot, F.; Crounse, J. D.; Kjaergaard, H. G.; Kroll, J. H.; Seinfeld, J. H.; Wennberg, P. O. Isoprene Photooxidation: New Insights into the Production of Acids and Organic Nitrates. *Atmos. Chem. Phys.* **2009**, *9* (4), 1479−1501.
(28) Møller, K. H.; Bates, K. H.; Kjaergaard, H. G. The Importance of Peroxy Radical Hydrogen-Shift Reactions in Atmospheric Isoprene Oxidation. *J. Phys. Chem. A* **2019**, *123* (4), 920−932.
(29) Berndt, T.; Hyttinen, N.; Herrmann, H.; Hansel, A. First Oxidation Products from the Reaction of Hydroxyl Radicals with Isoprene for Pristine Environmental Conditions. *Commun. Chem.* **2019**, *2* (1), 21.
(30) Peng, Z.; Lee-Taylor, J.; Orlando, J. J.; Tyndall, G. S.; Jimenez, J. L. Organic Peroxy Radical Chemistry in Oxidation Flow Reactors and Environmental Chambers and Their Atmospheric Relevance. *Atmos. Chem. Phys.* **2019**, *19* (2), 813−834.
(31) Peeters, J.; L. Nguyen, T.; Vereecken, L. HO X Radical Regeneration in the Oxidation of Isoprene. *Phys. Chem. Chem. Phys.* **2009**, *11* (28), 5935−5939.
(32) Bianchi, F.; Garmash, O.; He, X.; Yan, C.; Iyer, S.; Rosendahl, I.; Xu, Z.; Rissanen, M. P.; Riva, M.; Taipale, R.; et al. Insight into Naturally-Charged Highly Oxidized Molecules (HOMs) in the Boreal Forest. *Atmos Chem. Phys. Discuss.* **2017**, *2017*, 1−20.
(33) Ehn, M.; Thornton, J. A.; Kleist, E.; Sipilä, M.; Junninen, H.; Pullinen, I.; Springer, M.; Rubach, F.; Tillmann, R.; Lee, B.; et al. A Large Source of Low-Volatility Secondary Organic Aerosol. *Nature* **2014**, *506* (7489), 476−479.
(34) Berndt, T.; Richters, S.; Jokinen, T.; Hyttinen, N.; Kurtén, T.; Otkjær, R. V.; Kjaergaard, H. G.; Stratmann, F.; Herrmann, H.; Sipilä, M.; et al. Hydroxyl Radical-Induced Formation of Highly Oxidized Organic Compounds. *Nat. Commun.* **2016**, *7*, 1−8.
(35) Xu, L.; Møller, K. H.; Crounse, J. D.; Otkjær, R. V.; Kjaergaard, H. G.; Wennberg, P. O. Unimolecular Reactions of Peroxy Radicals Formed in the Oxidation of α-Pinene and β-Pinene by Hydroxyl Radicals. *J. Phys. Chem. A* **2019**, *123* (8), 1661−1674.
(36) Wennberg, P. O.; Bates, K. H.; Crounse, J. D.; Dodson, L. G.; McVay, R. C.; Mertens, L. A.; Nguyen, T. B.; Praske, E.; Schwantes, R. H.; Smarte, M. D.; et al. Gas-Phase Reactions of Isoprene and Its Major Oxidation Products. *Chem. Rev.* **2018**, *118*, 3337−3390.
(37) Teng, A. P.; Crounse, J. D.; Wennberg, P. O. Isoprene Peroxy Radical Dynamics. *J. Am. Chem. Soc.* **2017**, *139* (15), 5367−5377.
(38) Wolfe, G. M.; Marvin, M. R.; Roberts, S. J.; Travis, K. R.; Liao, J. The Framework for 0-D Atmospheric Modeling (F0AM) v3.1. *Geosci. Model Dev.* **2016**, *9* (9), 3309−3319.
(39) Jenkin, M. E.; Young, J. C.; Rickard, A. R. The MCM v3.3.1 Degradation Scheme for Isoprene. *Atmos. Chem. Phys.* **2015**, *15* (20), 11433−11459.
(40) Liu, Z.; Son Nguyen, V.; Harvey, J.; Müller, J.-F.; Peeters, J. The Photolysis of α-Hydroperoxycarbonyls. *Phys. Chem. Chem. Phys.* **2018**, *20* (10), 6970−6979.
(41) Liu, Z.; Son Nguyen, V.; Harvey, J.; Müller, J.-F.; Peeters, J. Theoretically Derived Mechanisms of HPALD Photolysis in Isoprene Oxidation. *Phys. Chem. Chem. Phys.* **2017**, *19* (13), 9096−9106.
(42) Sheps, L.; Rotavera, B.; J. Eskola, A.; L. Osborn, D.; A. Taatjes, C.; Au, K.; E. Shallcross, D.; H. Khan, M. A.; J. Percival, C. The Reaction of Criegee Intermediate CH 2 OO with Water Dimer: Primary Products and Atmospheric Impact. *Phys. Chem. Chem. Phys.* **2017**, *19* (33), 21970−21979.
(43) Jenkin, M. E.; Hurley, M. D.; Wallington, T. J. Investigation of the Radical Product Channel of the CH3OCH2O2 + HO2 Reaction in the Gas Phase. *J. Phys. Chem. A* **2010**, *114* (1), 408−416.
(44) Shaw, M. F.; Sztáray, B.; Whalley, L. K.; Heard, D. E.; Millet, D. B.; Jordan, M. J. T.; Osborn, D. L.; Kable, S. H. Photo-Tautomerization of Acetaldehyde as a Photochemical Source of Formic Acid in the Troposphere. *Nat. Commun.* **2018**, *9* (1), 2584−2591.
(45) Lei, X.; Wang, W.; Cai, J.; Wang, C.; Liu, F.; Wang, W. Atmospheric Chemistry of Enols: Vinyl Alcohol + OH + O2 Reaction Revisited. *J. Phys. Chem. A* **2019**, *123* (14), 3205−3213.
(46) Assaf, E.; Sheps, L.; Whalley, L. K.; Heard, D. E.; Tomas, A.; Schoemaecker, C.; Fittschen, C. The Reaction between CH3O2 and OH Radicals: Product Yields and Atmospheric Implications. *Environ. Sci. Technol.* **2017**, *51*, 2170−2177.
(47) Assaf, E.; Schoemaecker, C.; Vereecken, L.; Fittschen, C. Experimental and Theoretical Investigation of the Reaction of RO2 Radicals with OH Radicals: Dependence of the HO2 Yield on the Size of the Alkyl Group. *Int. J. Chem. Kinet.* **2018**, *50* (9), 670−680.
(48) Peeters, J.; Müller, J.-F.; Stavrakou, T.; Nguyen, V. S. Hydroxyl Radical Recycling in Isoprene Oxidation Driven by Hydrogen Bonding and Hydrogen Tunneling: The Upgraded LIM1Mechanism. *J. Phys. Chem. A* **2014**, *118* (38), 8625−8643.
(49) Butkovskaya, N. I.; Pouvesle, N.; Kukui, A.; Mu, Y.; Le Bras, G. Mechanism of the OH-Initiated Oxidation of Hydroxyacetone over

https://dx.doi.org/10.1021/acsearthspacechem.0c00010
ACS Earth Space Chem. 2020, 4, 730−740

the Temperature Range 236−298 K. *J. Phys. Chem. A* **2006**, *110* (21), 6833−6843.
(50) Kaiser, J.; Skog, K. M.; Baumann, K.; Bertman, S. B.; Brown, S. B.; Brune, W. H.; Crounse, J. D.; de Gouw, J. A.; Edgerton, E. S.; Feiner, P. A.; et al. Speciation of OH Reactivity above the Canopy of an Isoprene-Dominated Forest. *Atmos. Chem. Phys.* **2016**, *16* (14), 9349−9359.
(51) Bates, K. H.; Jacob, D. J. A New Model Mechanism for Atmospheric Oxidation of Isoprene: Global Effects on Oxidants, Nitrogen Oxides, Organic Products, and Secondary Organic Aerosol. *Atmos. Chem. Phys.* **2019**, *19* (14), 9613−9640.

https://dx.doi.org/10.1021/acsearthspacechem.0c00010
ACS Earth Space Chem. 2020, 4, 730−740